

# Changes and characteristics of dissolved organic matter in a constructed wetland system using fluorescence spectroscopy

Yuan Yao<sup>1</sup> · Yun-zhen Li<sup>2</sup> · Xu-jing Guo<sup>3,4</sup> · Tao Huang<sup>1</sup> · Ping-ping Gao<sup>1</sup> · Ying-pei Zhang<sup>1</sup> · Feng Yuan<sup>1</sup>

Received: 22 July 2015 / Accepted: 7 March 2016 / Published online: 15 March 2016  
© Springer-Verlag Berlin Heidelberg 2016

**Abstract** Domestic wastewater was treated by five constructed wetland beds in series. Dissolved organic matter (DOM) collected from influent and effluent samples from the constructed wetland was investigated using fluorescence spectroscopy combined with fluorescence regional integration (FRI), parallel factor (PARAFAC) analysis, and two-dimensional correlation spectroscopy (2D-COS). This study evaluates the capability of these methods in detecting the spectral characteristics of fluorescent DOM fractions and their changes in constructed wetlands. Fluorescence excitation–emission matrix (EEM) combined with FRI analysis showed that protein-like materials displayed a higher removal ratio compared to humic-like substances. The PARAFAC analysis of wastewater DOM indicated that six fluorescent components, i.e., two protein-like substances (C1 and C6), three

humic-like substances (C2, C3 and C5), and one non-humic component (C4), could be identified. Tryptophan-like C1 was the dominant component in the influent DOM. The removal ratios of six fluorescent components (C1–C6) were 56.21, 32.05, 49.19, 39.90, 29.60, and 45.87 %, respectively, after the constructed wetland treatment. Furthermore, 2D-COS demonstrated that the sequencing of spectral changes for fluorescent DOM followed the order 298 nm → 403 nm → 283 nm (310–360 nm) in the constructed wetland, suggesting that the peak at 298 nm is associated with preferential tryptophan fluorescence removal. Variation of the fluorescence index (FI) and the ratio of fluorescence components indicated that the constructed wetland treatment resulted in the decrease of fluorescent organic pollutant with increasing the humification and chemical stability of the DOM.

Responsible editor: Philippe Garrigues

**Electronic supplementary material** The online version of this article (doi:10.1007/s11356-016-6435-5) contains supplementary material, which is available to authorized users.

✉ Xu-jing Guo  
gxj530520@126.com

<sup>1</sup> Faculty of Geosciences and Environmental Engineering, Southwest Jiaotong University, Chengdu 610031, People's Republic of China

<sup>2</sup> Sichuan Academy of Environmental Sciences Sichuan, Chengdu 610041, People's Republic of China

<sup>3</sup> Key Laboratory of Development and Application of Rural Renewable Energy, Ministry of Agriculture, Biogas Institute of Ministry of Agriculture, No.13 Sec 4 Renmin Road South, Chengdu 610041, People's Republic of China

<sup>4</sup> Present address: College of Resources and Environment, Chengdu University of Information Technology, No.24 Block 1, Xuefu Road, Chengdu 610225, People's Republic of China

**Keywords** Dissolved organic matter · Constructed wetland · Fluorescence excitation–emission matrix · Fluorescence regional integration · Parallel factor analysis · Two-dimensional correlation spectroscopy

## Introduction

Constructed wetlands are designed to remove pollutants from contaminated water within a more controlled environment by utilizing natural processes, including sedimentation, filtration, precipitation, volatilization, adsorption, plant uptake, and various microbial processes (Faulwetter et al. 2009). Constructed wetlands have several advantages over classical activated sludge systems, including low external energy requirements and operation costs, and lower—sometimes even the absence of—sludge production (Vymazal 2009; Ayaz et al. 2015). These advantages make constructed wetlands suitable for the treatment of various wastewaters (e.g., agricultural effluents,

industrial wastewater, and aquaculture waters). Many studies have reported the removal of nitrogen, phosphorus, and chemical oxygen demand (COD) (Zou et al. 2009; Li et al. 2011; Zhang et al. 2015), but rarely have they studied changes in dissolved organic matter (DOM) in constructed wetlands.

DOM consists of a complex mixture of organic compounds and can be used to assess water quality (Coble 2007; Yamashita and Jaffé 2008). The presence and characteristics of DOM in domestic wastewater are of great interest with respect to constructed wetlands (Du et al. 2014), and its structure, composition, and relative abundance can influence its degradation capability in wastewater treatment processes. Characterization of DOM therefore plays an important role in understanding and managing constructed wetlands.

Spectroscopic techniques, especially fluorescence spectroscopy, provide information about the source and composition of DOM (Coble 1996; Stedmon et al. 2011; Guo et al. 2014). Synchronous fluorescence spectroscopy provides improved peak resolution and increased selectivity or structural signatures among the various DOM components, compared to the conventional fluorescence methods (Chen et al. 2003a, b). Fluorescence excitation–emission matrices (EEMs) are considered a useful tool for distinguishing among different types and sources of DOM in marine ecosystems (Lønborg et al. 2010; Kowalczyk et al. 2013), freshwater sources (Fellman et al. 2010), and water treatment systems (Baghoth et al. 2011).

Because of the heterogeneous nature of DOM and its complex chemical structure, however, significant spectral overlapping and peak shifting and broadening often occur, making the identification and interpretation of spectral signatures difficult. Therefore, various methods have been applied to the analysis of fluorescence spectra. The fluorescence index (FI) is calculated as the ratio of emission intensity at 450 and 500 nm, at 370-nm excitation, and has been used to distinguish microbially derived DOM sources from terrestrially derived sources (McKnight et al. 2001). The peak intensity ratios could provide additional information about the origin and structure of the biological macromolecules (Sheng and Yu 2006). More recently, fluorescence regional integration (FRI) has also been used to characterize DOM and to quantitatively analyze all the wavelength-dependent fluorescence intensity data from EEM spectra (Chen et al. 2003a, 2003b; Yu et al. 2011; He et al. 2011). In addition, parallel factor (PARAFAC) analysis identifies fluorescing components in the DOM of aquatic environments (Kowalczyk et al. 2009). The PARAFAC model may be an ideal technique for resolving the spectral overlapping of DOM. EEM-PARAFAC, combined with principal component analysis (PCA) scores, has shown that the differences in geology and associated land use control the dynamics of chromophoric DOM (Yao et al. 2011). Furthermore, two-dimensional correlation spectroscopy (2D-COS) has been applied to simplify complex spectra consisting of many overlapped peaks, and enhances the

spectral resolution by extending peaks along a two-dimensional space (Noda and Ozaki 2004). 2D-COS allows one to easily identify the sequential order of any subtle spectral change arising from external perturbations (e.g., pressure, temperature, or concentration variations) over a two-dimensional correlation map. Hur and Lee (2011) utilized 2D-COS and synchronous fluorescence spectra to present the molecular heterogeneity of DOM fractions.

In this study, domestic wastewater was treated in five constructed wetland beds in series. The EEM spectra, combined with PARAFAC and FRI, were used to identify fluorescent (e.g., protein-like, fulvic-like, and humic-like) components, and to observe the resulting changes that occur in the DOM of constructed wetlands. The 2D-COS and synchronous fluorescence spectra can be used to analyze the sequential order of any subtle spectral change arising from external perturbations. Our objective was to evaluate the capability of these methods in detecting changes in fluorescent DOM fractions in constructed wetlands.

## Materials and methods

### Sample collection

Water samples for this study were collected from five constructed wetland beds in a series in the Ergou constructed wetland of the Fenghuang River. This constructed wetland system consists of a primary biological pond, primary plant gravel beds, a secondary biological pond, secondary plant gravel beds, and a sand plant filter. A constructed rapid infiltration system was used for the preliminary treatment of the constructed wetland. Wastewater passed through five wetland beds. Influent and effluent water samples were collected from a water intake (I1) and from five water outlets (E1–E5). Immediately after collection, the DOM samples were filtered through a pre-combusted (5 h at 450 °C) 0.45- $\mu\text{m}$  PTFE membrane filter. All the samples were stored in the dark at 4 °C in pre-combusted amber glass vials until analysis. DOC concentrations of all the pre-filtered samples were determined using the combustion and non-dispersed infrared methods, utilizing a total organic carbon (TOC) analyzer (multi N/C 2100, Analytikjena, Germany).

### Spectral measurements

Fluorescence EEM spectra were measured with a Hitachi F-7000 spectrofluorometer (Hitachi, Japan) equipped with a 150-W Xenon arc lamp as the light source. EEM spectra were obtained by scanning the emission spectra from 280 to 550 nm by incrementing the excitation wavelength at 5-nm intervals, from 200 to 450 nm. The spectra were recorded at a scan rate of 1200 nm min<sup>-1</sup> using excitation and emission slit bandwidths of 5 nm. The fluorescence response to a neutral

solution (Milli-Q water) was subtracted from the spectra of each sample, to eliminate Raman scattering effects (McKnight et al. 2001; Lawaetz and Stedmon 2009). Synchronous fluorescence spectra were recorded for samples with a constant offset ( $\Delta\lambda=55$  nm) between excitation and emission wavelengths, at 5-nm slit widths. The scan speed, spectral range, and response time were set to  $240 \text{ nm min}^{-1}$ , 250–550 nm, and auto, respectively. Several different offset values were initially investigated. We chose to use  $\Delta\lambda=55$  nm because it obtained the most significant differences in the spectra DOM samples.

**PARAFAC modeling**

The PARAFAC method of analyzing EEMs has been described in the literature (Bro 1997). This analysis was carried out in Matlab 7.0 software using the DOMFluor toolbox. PARAFAC was applied to our EEM dataset (96 samples  $\times$  55 emissions  $\times$  47 excitations) with some analytical and statistical assumptions as reported by Stedmon and Bro (2008). PARAFAC models with three to seven components were computed for the EEMs. Determination of the correct number of components was based on split-half analysis, residual analysis, and visual inspection (Stedmon and Bro 2008). The sum of squared residuals in the excitation and emission scans is plotted in Supplementary Fig. S1. It seems clear that the step from six to seven component models offered little improvement in fit, suggesting that six or fewer components were adequate for this data (Supplementary Fig. S1). Split-half analysis compares the excitation and emission loadings of the models run on separate splits of the data using Tucker congruence coefficients (Lorenzo-Seva and Berge 2006) and indicates whether the model is validated. We found that six components can be split-half-validated and that they accounted for 99.0393 % of the variance. Therefore, six components could be identified using the PARAFAC models.  $F_{\text{max}}$  then gave estimates of the relative abundance of each component.

**Regional integration analysis**

In this study, the EEM was divided into five regions: region I, tyrosine-like materials, excitation/emission (Ex/Em)  $<250 \text{ nm}/<330 \text{ nm}$ ; region II, tryptophan-like materials, Ex/Em  $<250 \text{ nm}/<380 \text{ nm}$ ; region III, fulvic-like materials, Ex/Em  $<250 \text{ nm}/>380 \text{ nm}$ ; region IV, soluble microbial by-product-like materials, Ex/Em  $>250 \text{ nm}/<380 \text{ nm}$ ; and region V, humic-like materials, Ex/Em  $>250 \text{ nm}/>380 \text{ nm}$ ) (Chen et al. 2003a, b). By normalizing the cumulative excitation–emission area volumes to relative regional areas ( $\text{nm}^2$ ), the normalized area volumes were calculated according to the literature (Chen et al. 2003a, b). The  $P_{i, n}$  value ( $I=I-V$ ) was used to represent the area volume of each region.

**Determination and analysis of 2D-COS**

2D-COS has been widely applied to resolve peak overlapping problems and to enhance the spectral resolution by extending peaks along a second dimension (Noda and Ozaki 2004; Hur and Lee 2011; Xu et al. 2013; Li et al. 2014). The theoretical basis of 2D-COS has also been illuminated by Ozaki et al. (2001). Hence, the reconstructed spectral data sets (synchronous and asynchronous) were transformed into a new spectral matrix suitable for 2D-COS mapping, using the “2D Shige” software released by Kwansei-Gakuin University (Nakashima et al. 2008).

**Statistical analyses**

The correlation and ANOVA analyses were performed using SPSS 16.0 software. Correlation analyses were used to examine the relationships among variables. Pearson’s correlation coefficient ( $r$ ) was used to evaluate the linear correlation between two parameters. Significance levels were reported as non-significant (NS;  $p>0.05$ ), significant (a,  $0.05>p>0.01$ ), or highly significant (b,  $p<0.01$ ). The linear regression model was used for all correlation analyses and was validated using analysis of variance (ANOVA).

**Table 1** Distribution of  $P_{i,n}$  ( $\times 10^6$ ,  $\text{aunm}^2 [\text{mg/L}]^{-1}$ ) of DOM sample from regional integrity analysis

Sample	$P_{I, n}$	$P_{II, n}$	$P_{III, n}$	$P_{IV, n}$	$P_{V, n}$	$P_p$	$P_h$	$P_p/P_h^a$	$P_{V, n}/P_{III, n}$
I1	0.318	0.653	1.478	3.858	9.055	4.829	10.533	2.181	6.127
E1	0.146	0.491	0.917	2.188	5.859	2.825	6.776	2.399	6.389
E2	0.123	0.351	0.887	1.762	5.544	2.236	6.431	2.876	6.250
E3	0.143	0.380	0.904	1.850	5.573	2.373	6.477	2.729	6.165
E4	0.136	0.358	0.893	1.985	5.836	2.479	6.729	2.714	6.535
E5	0.126	0.321	0.764	1.785	5.171	2.232	5.935	2.659	6.768

<sup>a</sup>  $P_h/P_p = \sum(III + V)/\sum(I + II + IV)$

**Table 2** The removal ratio (%) of  $P_{i,n}$  in the constructed wetland beds

Sample	$P_{I,n}$	$P_{II,n}$	$P_{III,n}$	$P_{IV,n}$	$P_{V,n}$	$\sum P_{i,n}$
I1/E1	54.09	24.81	37.96	43.29	35.30	37.50
E1/E2	15.75	28.51	3.27	19.47	5.38	9.73
E2/E3	-16.26	-8.26	-1.92	-4.99	-0.52	-2.11
E3/E4	4.90	45.18	39.58	48.55	35.55	40.06
E4/E5	7.35	10.34	14.45	10.08	11.39	11.31
I1/E5	60.38	50.84	48.31	53.73	42.89	46.84

## Results and discussion

### Fluorescence EEM spectra with regional integration analysis

The distribution of  $P_{i,n}$  in the DOM samples from the regional integration analysis is listed in Table 1. The  $P_{i,n}$  values suggested a dramatic decrease of fluorescent organic matter in the effluents compared to those in the influents, indicating that fluorescent organic matter was removed by the constructed wetland. However, Table 1 demonstrated that the  $P_{i,n}$  values from regions I–V in the E2 sample were lower than those in the other effluents. The  $P_{i,n}$  values from these regions in the E3 sample showed a slight increase over those in the E2. The removal of organic matter in constructed wetlands is complex and depends on a variety of removal mechanisms, including sedimentation, filtration, precipitation, volatilization, adsorption, plant uptake, and various microbial processes (Vymazal 2009). These processes generally directly and/or indirectly influence the production and degradation of DOM.

The  $P_p$  values in the influent were markedly lower compared to the  $P_h$  values (Table 1). Regions III and V suggested the presence of aromatic organic compounds, which have a higher degree of aromatic polycondensation and chemical stability (Santos et al. 2010). Senesi et al. (2003) suggested that the broader excitation and emission bands, and the longer emission wavelength, in region V, were associated with humic substances composed of high-molecular-weight aromatic organic compounds. The ratio  $P_h/P_p$  can indicate changes in the DOM structure.  $P_h/P_p$  suggested a marked increase in the effluent DOM compared to that in the influent. The  $P_{V,n}/P_{III,n}$  value was used to assess the humification degree of the DOM. Similarly, the  $P_{V,n}/P_{III,n}$  values increased markedly in the effluent DOM compared to those in the influents, suggesting an increase in the humification degree.

Table 2 shows the changes in the removal ratios in the five constructed wetland beds. Fluorescent DOM indicated a marked decrease in the first constructed wetland bed. The removal ratios for regions I, II, and IV varied in the order  $P_{I,n} > P_{IV,n} > P_{II,n}$ , suggesting that labile protein-like material (region I) was degraded easily by the constructed wetland beds. The removal ratios of  $P_{V,n}$  with a high degree of aromatic polycondensation and chemical stability were relatively lower than those of  $P_{III,n}$ . Although  $P_{i,n}$  values demonstrate an obvious increase in the E3 compared to those in the E2, they also can be removed sequentially in the subsequent wetland beds. The removal ratios of  $P_{i,n}$  for all regions varied in the order  $P_{I,n} > P_{IV,n} > P_{II,n} > P_{III,n} > P_{V,n}$  in the I1/E5, indicating that protein-like materials displayed higher removal ratios compared to the humic-like substances.

**Fig. 1** Six different fluorescent components identified by the PARAFAC model from the influent and effluent DOM in constructed wetland

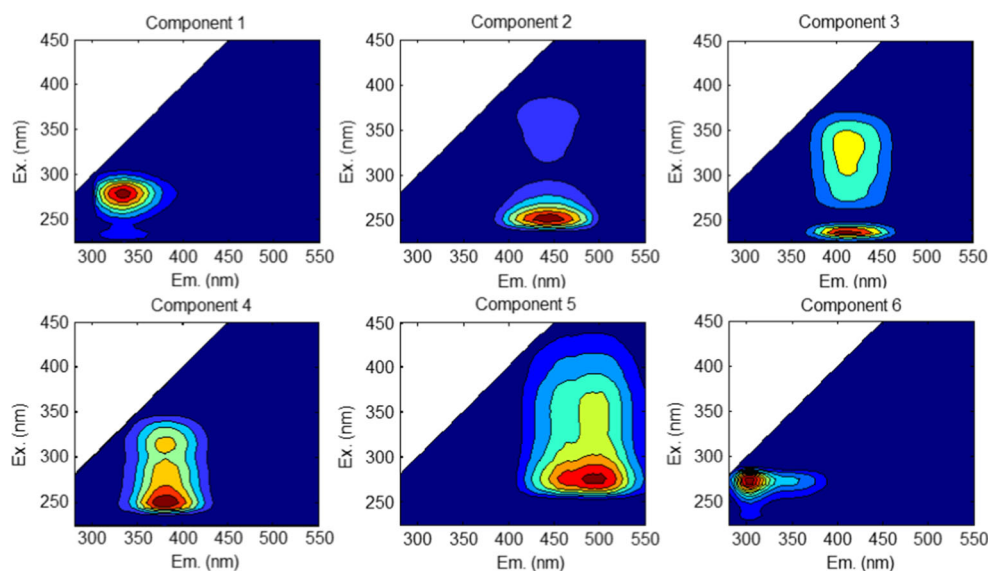




**Table 3** Descriptions of the six components identified by PARAFAC analysis in this study

Fluorescent component	Excitation/emission wavelength	Description and source assignment
C1	234(280)/335	Tryptophan-like fluorescence; autochthonous origin
C2	250(360)/440	Humic-like; terrestrial origin
C3	235(335)/410	Traditionally fulvic-like fluorescence peak A; terrestrial origin
C4	245(315)/375	Non-Humic-like; labile matter; biological production in the water column N-peak
C5	280(345)/500	Soil fulvic-like; derived from agricultural catchments and exists in freshwater environments soil-fulvic-acid
C6	230(275)/305	Tyrosine-like fluorescence; autochthonous origin

**Changes in the EEM-PARAFAC components of DOM**

Although regional integration analysis can be used to quantitatively analyze EEM spectra and to determine the configuration and heterogeneity of DOM, the traditional “peak picking” technique is problematic for interpreting the multi-dimensional nature of EEM datasets due to the overlapping of the various fluorescence peaks (Maie et al. 2007; Yamashita et al. 2010). The EEM spectra, combined with PARAFAC, however, provide higher resolution on EEM fluorescence components in DOM than the traditional peak picking technique. This approach was therefore used to detect variations in DOM composition in the constructed wetland. In this study, six individual components (C1–C6) were validated for this dataset using the PARAFAC model (Fig. 1), i.e., two protein-like substances (components 1 and 6), three humic-like substances (components 2, 3, and 5), and one non-humic component (component 4). Supplementary Figs. S2 and S3 show the excitation and emission loadings and the split-half analysis identified by PARAFAC models.

As shown in Table 3, component C1 was composed of two peaks with the excitation maxima at 234 and 280 nm and the emission wavelength at 335 nm, which was related to an autochthonous tryptophan-like fluorescence. This component is a typical protein-like substance that can be observed in both marine (Coble 1996; Murphy et al. 2008; Kowalczyk et al. 2009) and terrestrial waters (Yao et al. 2011; Guo et al. 2014)

Component C2 exhibited primary (and secondary) fluorescence peaks at an excitation/emission wavelength pair of 250 (360) nm/440 nm. This component was also similar to the traditional terrestrial humic-like peak C (Coble 1996), whereas component C1 was expected to consist of compounds that are more hydrophobic and larger in molecular weight units (Ishii and Boyer 2012).

Component C3 had a primary fluorescence peak at an Ex/Em wavelength pair of 235 nm/410 nm and a secondary peak at 335 nm/410 nm, which were similar to the traditionally terrestrial fulvic-like fluorescence peak A (Coble 1996; Kowalczyk et al. 2009), and to the PARAFAC components

of terrestrial humic-like materials (Murphy et al. 2008; Yuan et al. 2015).

A blue shift can be observed for C4, with respect to C2 and C3, fluorescing at a primary (secondary) excitation/emission wavelength pair of 245 (315) nm/375 nm. This component is similar to a non-humic substance and lies between tryptophan and an N-peak (Coble et al. 1998), which could be a combination of a tryptophan-like substance (peak T) (Coble 1996) and biologically labile matter produced in aquatic environments (Singh et al. 2010). C4 was reported as a non-humic component of freshly produced biologically labile material (Yamashita and Jaffé 2008) and a protein- or amino-acid-like component (Kowalczyk et al. 2009).

Compared with the humic-like components C2 and C3, component C5 suggested a marked red shift, composed of two excitation maxima, at 280 and 345 nm, both with the emission maximum centered at 500 nm. The spectral features were also similar to soil-derived humic acid originating from wetlands and marshes (Singh et al. 2010; Yuan et al. 2015). Stedmon and Markager (2005) have reported that this

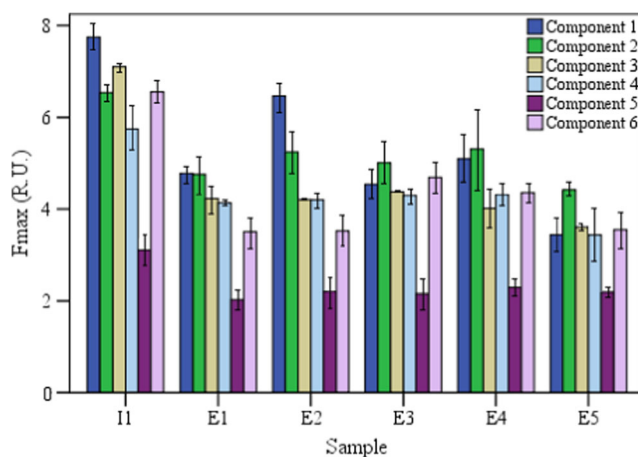


**Fig. 2** Changes of PARAFAC-derived DOM components for influent and effluents in the constructed wetland

**Table 4** The removal ratio (%) of fluorescent component in the constructed wetland beds

Sample	Component 1	Component 2	Component 3	Component 4	Component 5	Component 6	$\Sigma$
I1/E1	38.35	27.27	40.42	28.04	34.66	46.46	36.30
E1/E2	-35.98	-10.23	0.55	-1.65	-8.26	-0.37	-10.37
E2/E3	30.05	4.50	-4.28	-2.36	2.03	-33.17	3.04
E3/E4	-12.13	-5.96	8.37	-0.30	-6.25	6.98	-1.21
E4/E5	33.40	16.24	10.24	19.98	4.39	18.67	18.72
I1/E5	56.21	32.05	49.19	39.90	29.60	45.87	43.92

component could also be attributed to the leaching processes from agricultural catchments, given the long residence time of water in these catchments.

Component C6 showed two excitation maxima at 230 and 275 nm at 305-nm emission loading, which was categorized as the previously defined autochthonous tyrosine-like fluorescence peak B. This component was also similar to autochthonous protein-like PARAFAC components (Murphy et al. 2008; Yamashita and Jaffé 2008; Yao et al. 2011).

Figure 2 describes the changes in the PARAFAC-derived DOM components for the influent and effluents in the five constructed wetland beds. Levels of tryptophan-like C1 were highest in the influent DOM, compared to other components. However, protein-like C6 also obtained a high  $F_{\max}$  value. C3 was a dominant humic-like component and accounted for 19.29 %. Terrestrial humic-like C5 showed a markedly low  $F_{\max}$  value and only accounted for 8.45 %.

As shown in Fig. 2, fluorescent components indicated a significant change in the influent DOM compared to the effluent DOM. However, the results were similar to those from regional integration analysis that fluorescent components showed an increase and/or a decrease in the effluents. A variety of removal mechanisms resulted in changes in the  $F_{\max}$  value. Table 4 shows the removal ratios of six components in the five constructed wetland beds. Through constructed wetland treatment, the removal ratios of fluorescent components

were 56.21, 32.05, 49.19, 39.90, 29.60, and 45.87 % for components 1–6, respectively. In addition, C3 also indicated a relatively higher removal ratio than other humic-like substances, suggesting that humic-like substances at short wavelengths were degraded more easily than those at long wavelengths. Due to the presence of recalcitrant characteristics, humic-like components 2 and 5 showed low removal efficiencies in the I1 and E5 samples, of 32.05 and 29.60 %, respectively. The presence of recalcitrant humic-like substances and the production of fluorescent organic matters led to a total removal ratio of fluorescent components ( $\Sigma$ ) of only 43.92 %. The results suggest that most of fluorescent components were removed in the first constructed wetland bed.

## 2D-COS

A synchronous map is symmetrical around the main diagonal, and the correlation peaks will appear in the main diagonal (autopeak) and off-diagonal (cross-peak) areas. Figure 3 indicates that the synchronous map showed two autopeaks (280 and 338 nm). An autopeak suggests the overall susceptibility of the corresponding spectral region to the change in spectral intensity, as an external perturbation is applied to the system (Noda and Ozaki 2004). The intensities of the autopeaks decreased in the order 280 nm  $\rightarrow$  338 nm, suggesting that they

**Fig. 3** Synchronous and asynchronous 2COS maps generated from synchronous fluorescence spectra of DOM in the constructed wetland. Red represents positive correlation, and blue represents negative correlation; a higher color intensity indicates a stronger positive or negative correlation

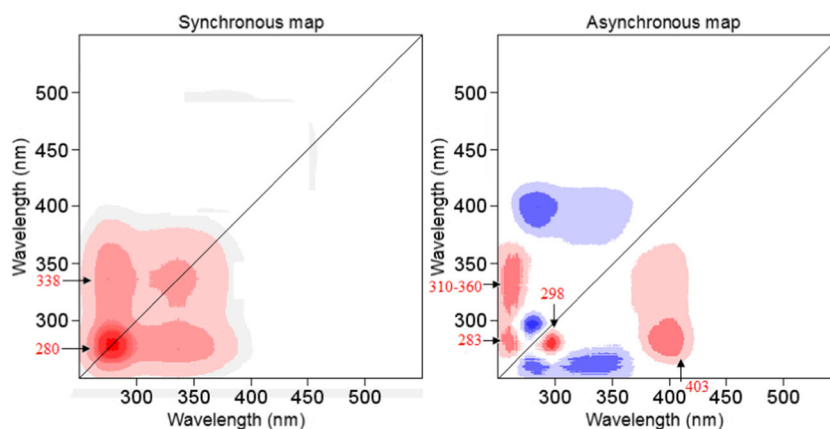


**Table 5** Variation of fluorescence index and the ratio of fluorescence components

Sample	FI	C1/C2	C1/C5	C6/C2	C6/C5	C2/C3	C5/C3
I1	2.322	1.185	2.494	1.002	2.110	0.922	0.438
E1	2.225	1.004	2.353	0.738	1.729	1.125	0.480
E2	2.187	1.239	2.956	0.672	1.603	1.247	0.523
E3	2.214	0.908	2.110	0.937	2.179	1.142	0.491
E4	2.165	0.960	2.227	0.822	1.907	1.321	0.570
E5	2.095	0.686	1.552	0.718	1.622	1.371	0.607

were more susceptible to the changes in protein-like fluorescence intensity at 280 nm. Off-diagonal peaks in the synchronous map exhibited a positive correlation at 338 nm. The results demonstrated that fulvic-like substances at short wavelengths were more susceptible to such changes than humic-like substances at long wavelengths.

The asynchronous map is anti-symmetrical around the diagonal line, showing no autopeaks and revealing the degree of the sequential changes at two different wavelengths (Hur and Lee 2011). Two positive and two negative peak areas were observed below the diagonal line ( $x_1$ ) of the asynchronous map. A negative peak area was placed at the  $x_1$  wavelength of 283 nm; this is an aromatic amino acid peak, indicative of a protein-like moiety in the DOM, specifically tyrosine (Barker et al. 2009). A positive peak at 298 nm is associated with tryptophan fluorescence (Yamashita and Tanoue 2003). Fulvic-like materials showed negative peak areas (310–360 nm) for  $x_1$ . A large positive peak area appeared at the  $x_1$  wavelength of 403 nm and was related to humic-like substances. According to Noda’s rule (Noda and Ozaki 2004), the degree of the sequential changes for fluorescent DOM components followed the order 298 nm → 403 nm → 283 nm (310–360 nm) in the constructed wetland.

### Spectroscopic indication of DOM evolution in the constructed wetland

The fluorescence indexes, FI, which are defined as the ratios of emission intensity at 450 and 500 nm at 370-nm excitation (McKnight et al. 2001), can be used as indicators of the relative contribution of DOM derived from terrestrial or microbial substances. FI values of 1 or greater (~1.9 or higher) correspond to freshly produced DOM of biological or microbial origin, whereas values of 1.4 and lower reflect organic matter of an allochthonous (terrestrial) origin. The FI values showed a marked decrease in the E5 outlet-area sample compared to those in the I1 intake-area sample (Table 5), suggesting a decrease in microbially derived organic matter. This result also demonstrated the removal of fluorescent organic pollutants, especially for protein-like materials.

The untreated wastewater (I1) had high levels of protein-like components (C1 and C6) compared with those of the effluents (Fig. 2). The ratio of protein-like components to visible humic-like components can be used as an indicator for input wastewater organic pollution in various aquatic environments (Guo et al. 2011). The ratios of C1/C2 and C6/C5 in the E5 sample were obviously lower than the corresponding ratios in the I1 sample, indicating a reduction in organic pollution. The peak shifts in the excitation wavelengths from shorter to longer indicated an increase in molecule size and aromatic content.

The intensity ratios could provide additional information about the chemical nature of the biological macromolecules (Sheng and Yu 2006). The ratios of C2/C3 and C5/C3 were markedly lower in the I1 sample than in the other samples, suggesting that the humification of DOM increased in the effluent DOM. Table 6 shows that FI was negatively correlated with C2/C3, C5/C3, and  $P_{V, n}/P_{III, n}$ , indicating that microbially derived DOM (e.g., protein-like material) gradually decreased with the increasing humification degree. C1/C2 was correlated with C1/C5 ( $r=0.968$ ,  $p<0.01$ ). C6/C2 was

**Table 6** Pearson correlation between the intensity ratios and the FRI parameters

	FI	C1/C2	C1/C5	C6/C2	C6/C5	C2/C3	C5/C3	$P_{V, n}/P_{III, n}$
FI	1.000	0.702	0.548	0.701	0.629	-0.975**	-0.960**	-0.848*
C1/C2		1.000	0.968**	0.146	0.112	-0.579	-0.666	-0.759
C1/C5			1.000	-0.042	-0.023	-0.411	-0.554	-0.696
C6/C2				1.000	0.962**	-0.714	-0.599	-0.574
C6/C5					1.000	-0.625	-0.569	-0.608
C2/C3						1.000	0.963**	0.807
C5/C3							1.000	0.889*
$P_{V, n}/P_{III, n}$								1.000

\*Correlation is significant at the 0.05 level (two-tailed); \*\*correlation is significant at the 0.01 level (two-tailed)

correlated with C6/C5 ( $r=0.962$ ,  $p<0.01$ ). C2/C3 was correlated with C5/C3 and  $P_{V, n}/P_{III, n}$  ( $r=0.963$ ,  $p<0.01$ , and  $r=0.889$ ,  $p<0.05$ , respectively). The above results suggested that organic pollution decreased with increasing humification and chemical stability of the DOM.

## Conclusions

Fluorescence EEM combined with regional integration analysis was used to assess the changes in fluorescent DOM. This method could be used as a valuable research tool for detecting the qualitative removal potentials of different fluorescent DOM fractions. Protein-like materials show a higher removal ratio compared to humic-like substances. The total removal ratio of the fluorescent DOM fractions was 46.84 %. The EEM spectra combined with PARAFAC provides higher resolution on EEM fluorescence components in DOM than the traditional peak picking technique. The EEM-PARAFAC revealed high concentrations of degradable protein-like components (C1 and C6). The results also showed that humic-like substances at short wavelengths were degraded more easily than those at long wavelengths. 2D-COS was used to analyze the sequential order of subtle spectral changes arising from external perturbations and to identify the sequence of the removals for fluorescent DOM. The degree of the sequential changes in fluorescent DOM components followed the order 298 nm  $\rightarrow$  403 nm  $\rightarrow$  283 nm (310–360 nm) in the constructed wetland. Use of the combined intensity ratios may provide a quantification tracer for the changes in DOM fractions and chemical stability. The humification of DOM increased in the effluent DOM, and microbially derived DOM gradually decreased with increasing humification degree in the constructed wetland.

**Acknowledgments** This work was financially supported by Public-Interest Scientific Institution Basal Research Fund of the Science & Technology Department of Sichuan Province (2013038–1) and the Returned Overseas Chinese Scholars Fund of Sichuan Province.

## References

- Ayaz SC, Akats Ö, Akca L, Findik N (2015) Effluent quality and reuse potential of domestic wastewater treated in a pilot-scale hybrid constructed wetland system. *J Environ Manage* 156:115–120
- Baghouth SA, Sharma SK, Amy GL (2011) Tracking natural organic matter (NOM) in a drinking water treatment plant using fluorescence excitation-emission matrices and PARAFAC. *Water Res* 45:797–809
- Barker JD, Sharp MJ, Turner RJ (2009) Using synchronous fluorescence spectroscopy and principal components analysis to monitor dissolved organic matter dynamics in a glacier system. *Hydrol Process* 23:1487–1500
- Bro R (1997) PARAFAC. tutorial and applications. *Chemom Intell Lab Syst* 38:149–171
- Chen J, LeBoeuf EJ, Dai S, Gu B (2003a) Fluorescence spectroscopic studies of natural organic matter fractions. *Chemosphere* 50:639–647
- Chen W, Westerhoff P, Leenheer JA, Booksh K (2003b) Fluorescence Excitation–emission matrix regional integration to quantify spectra for dissolved organic matter. *Environ Sci Technol* 37:5701–5710
- Coble PG (1996) Characterization of marine and terrestrial DOM in seawater using excitation–emission matrix spectroscopy. *Mar Chem* 51:325–346
- Coble PG (2007) Marine optical biogeochemistry: the chemistry of ocean color. *Chem Rev* 107:402–418
- Coble PG, Del Castillo CE, Avril B (1998) Distribution and optical properties of CDOM in the Arabian Sea during the 1995 Southwest Monsoon. *Deep-Sea Res. II* 45:2195–2223
- Du X, Xu Z, Li J, Zheng L (2014) Characterization and removal of dissolved organic matter in a vertical flow constructed wetland. *Ecol Eng* 73:610–615
- Faulwetter JL, Gagnon V, Sundberg C, Chazarenc F, Burr MD, Brisson J, Camper AK, Stein OR (2009) Microbial processes influencing performance of treatment wetlands: a review. *Ecol Eng* 35:987–1004
- Fellman JB, Hood E, Spencer RGM (2010) Fluorescence spectroscopy opens new windows into dissolved organic matter dynamics in freshwater ecosystems: a review. *Limnol Oceanogr* 55:2452–2462
- Guo X, He L, Li Q, Yuan D, Deng Y (2014) Investigating the spatial variability of dissolved organic matter quantity and composition in Lake Wuliangshai. *Ecol Eng* 62:93–101
- Guo W, Xu J, Wang J, Wen Y, Zhuo J, Yan Y (2011) Characterization of dissolved organic matter in urban sewage using excitation emission matrix fluorescence spectroscopy and parallel factor analysis. *J Environ Sci* 22:1728–173
- He X, Xi B, Wei Z, Jiang Y, Yang Y, An D, Cao J, Liu H (2011) Fluorescence excitation–emission matrix spectroscopy with regional integration analysis for characterizing composition and Transformation of dissolved organic matter in landfill leachates. *J Hazard Mater* 190:293–299
- Hur J, Lee B (2011) Characterization of binding site heterogeneity for copper within dissolved organic matter fractions using two-dimensional correlation fluorescence spectroscopy. *Chemosphere* 83:1603–1611
- Ishii SKL, Boyer TH (2012) Behavior of reoccurring PARAFAC components in fluorescent dissolved organic matter in natural and engineered systems: a critical review. *Environ Sci Technol* 46:2006–2017
- Kowalczyk P, Tilstone GH, Zablocka M, Röttgers R, Thomas R (2013) Composition of dissolved organic matter along an Atlantic meridional transect from fluorescence spectroscopy and parallel factor analysis. *Mar Chem* 157:170–184
- Kowalczyk P, Cooper WJ, Durako MJ, Kahn AE, Gonsior M (2009) Characterization of dissolved organic matter fluorescence in the South Atlantic Bight with use of PARAFAC model: interannual variability. *Mar Chem* 113:182–196
- Lawaetz AJ, Stedmon CA (2009) Fluorescence intensity calibration using the raman scatter peak of water. *Appl Spectrosc* 63:936–940
- Li X, Dai X, Takahashi J, Li N, Jin J, Dai L, Dong B (2014) New insight into chemical changes of dissolved organic matter during anaerobic digestion of dewatered sewage sludge using EEM-PARAFAC and two-dimensional FTIR correlation spectroscopy. *Bioresour Technol* 159:412–420
- Li Y, Li H, Sun T, Wang X (2011) Study on nitrogen removal enhanced by shunt distributing wastewater in a constructed subsurface infiltration system under intermittent operation mode. *J Hazard Mater* 189:336–34
- Lønborg C, Álvarez-Salgado XA, Davidson K, Martínez-García S, Teira E (2010) Assessing the microbial bioavailability and degradation



- rate constants of dissolved organic matter by fluorescence spectroscopy in the coastal upwelling system of the Ría de Vigo. *Mar Chem* 119:121–129
- Lorenzo-Seva U, Berge JMFT (2006) Tucker's Congruence Coefficient as a meaningful index of factor similarity. *Methodology* 2:57–64
- Maie N, Scully NM, Pisani O, Jaffé R (2007) Composition of a protein-like fluorophore of dissolved organic matter in coastal wetland and estuarine ecosystems. *Water Res* 41:563–570
- McKnight DM, Boyer EW, Westerhoff PK, Doran PT, Kulbe T, Andersen DT (2001) Spectrofluorometric characterization of dissolved organic matter for indication of precursor organic material and aromaticity. *Limnol Oceanogr* 46:38–48
- Murphy KR, Stedmon CA, Waite TD, Ruiz G (2008) Distinguishing between terrestrial and autochthonous organic matter sources in marine environments using fluorescence spectroscopy. *Mar. Chem* 108:40–58
- Nakashima K, Xing S, Gong Y, Miyajima T (2008) Characterization of humic acids by two-dimensional correlation fluorescence spectroscopy. *J Mol Struct* 883–884:155–159
- Noda I, Ozaki Y (2004) Two-Dimensional correlation spectroscopy-applications in vibrational and optical spectroscopy. John Wiley and Sons Inc., London
- Ozaki Y, Czarnik-Matuszewicz B, Šašić S (2001) Two-dimensional correlation spectroscopy in analytical chemistry. *Anal Sci* 17:i663–i666
- Santos LM, Simões ML, Melo WJ, Martin-Neto L, PereiraFilho ER (2010) Application of chemometric methods in the evaluation of chemical and spectroscopic data on organic matter from Oxisols in sewage sludge applications. *Geoderma* 155:121–127
- Senesi N, D'Orazio V, Ricca G (2003) Humic acids in the first generation of eurosols. *Geoderma* 116:325–344
- Sheng GP, Yu HQ (2006) Characterization of extracellular polymeric substances of aerobic and anaerobic sludge using three-dimensional excitation and emission matrix fluorescence spectroscopy. *Water Res* 40:1233–1239
- Singh S, D'Sa EJ, Swenson EM (2010) Chromophoric dissolved organic matter (CDOM) variability in Barataria Basin using excitation–emission matrix (EEM) fluorescence and parallel factor analysis (PARAFAC). *Sci Total Environ* 408:3211–3222
- Stedmon CA, Bro R (2008) Characterizing dissolved organic matter fluorescence with parallel factor analysis: a tutorial. *Limnol Oceanogr Methods* 6:572–579
- Stedmon CA, Markager S (2005) Tracing the production and degradation of autochthonous fractions of dissolved organic matter using fluorescence analysis. *Limnol Oceanogr* 50:1415–26
- Stedmon CA, Seredyńska-Sobecka B, Boe-Hansen R, Tallec NL, Waul CK, Arvin E (2011) A potential approach for monitoring drinking water quality from groundwater systems using organic matter fluorescence as an early warning for contamination events. *Water Res* 45:6030–6038
- Vymazal J (2009) The use constructed wetlands with horizontal subsurface flow for various types of wastewater. *Ecol Eng* 35:1–17
- Xu H, Yu G, Yang L, Jiang H (2013) Combination of two-dimensional correlation spectroscopy and parallel factor analysis to characterize the binding of heavy metals with DOM in lake sediments. *J Hazard Mat* 263:412–421
- Yamashita Y, Jaffé R (2008) Characterizing the interactions between trace metals and dissolved organic matter using excitation emission matrix and parallel factor analysis. *Environ Sci Technol* 42:7374–7379
- Yamashita Y, Maie N, Briceno H, Jaffé R (2010) Optical characterization of dissolved organic matter in tropical rivers of the Guayana Shield, Venezuela. *J Geophys Res Biogeol* 115:G00F10. doi:10.1029/2009JG000987
- Yamashita Y, Tanoue E (2003) Chemical characterization of protein-like fluorescences in DOM in relation to aromatic amino acids. *Mar Chem* 82:255–271
- Yao X, Zhang Y, Zhu G, Qin B, Feng L, Cai L, Gao G (2011) Resolving the variability of CDOM fluorescence to differentiate the sources and fate of DOM in Lake Taihu and its tributaries. *Chemosphere* 82:145–155
- Yu G, Wu M, Luo Y, Yang X, Ran W, Shen Q (2011) Fluorescence excitation–emission spectroscopy with regional integration analysis for assessment of compost maturity. *Waste Manage* 31:1729–1736
- Yuan D, Guo X, Wen L, He L, Wang J, Li J (2015) Detection of copper (II) and cadmium (II) binding to dissolved organic matter from macrophyte decomposition by fluorescence excitation-emission matrix spectra combined with parallel factor analysis. *Environ Pollut* 204:152–160
- Zhang L, Ye Y, Wang L, Xi B, Wang H, Li Y (2015) Nitrogen removal processes in deep subsurface wastewater infiltration systems. *Ecol Eng* 77: 275–283
- Zou JL, Dai Y, Sun TH, Li YH, Li GB, Li QY (2009) Effect of amended soil and hydraulic load on enhanced biological nitrogen removal in lab-scale SWIS. *J Hazard Mater* 136: 816–822